Two New Antiferromagnetic Nickel(II) Complexes Bridged by Azido Ligands in the *Cis* Position. Effect of the Counteranion on the Crystal Structure and Magnetic Properties

Joan Ribas,*[1a] Montserrat Monfort,[1a] Barindra Kumar Ghosh,[1b] Roberto Cortés,[1c] Xavier Solans,[1d] and Mercé Font-Bardía[1d]

Departament de Química Inorgànica, Universitat de Barcelona, Diagonal 647, 08028 Barcelona, Spain, and Departament de Cristal.lografia i Mineralogia, Universitat de Barcelona, Martí i Franqués, s/n, 08028 Barcelona, Spain

Received August 10, 1995[⊗]

Two new nickel(II) end-to-end azido-bridged compounds, *cis-catena*-$[NiL_2(\mu\text{-}N_3)]_n(ClO_4)_n \cdot nH_2O$ (**1**) and $[Ni_2L_4(\mu\text{-}N_3)_2](PF_6)_2$ (**2**), were synthesized and characterized; L is 2-(aminoethyl)pyridine. The crystal structures of **1** and **2** were solved. Complex **1**: monoclinic system, space group $P2_1/a$, $a = 8.637(2)$ Å, $b = 18.9995(7)$ Å, $c = 12.3093(7)$ Å, $\beta = 105.92(2)°$, $Z = 4$. Complex **2**: triclinic system, space group $P\bar{1}$, $a = 9.139(7)$ Å, $b = 10.124(3)$ Å, $c = 12.024(2)$ Å, $\alpha = 70.407(14)°$, $\beta = 84.19(2)°$, $\gamma = 67.67(4)°$, $Z = 1$. In the two complexes the nickel atom is situated in a similarly distorted octahedral environment. The two complexes are different; **1** is a one-dimensional helicoidal complex with the two L ligands and the two end-to-end azido bridges in a *cis* arrangement while complex **2** is a dinuclear system with two end-to-end azido bridges, indicating the extreme importance of the counteranion present (ClO_4^- for **1** and PF_6^- for **2**). The magnetic properties of the two compounds were studied by susceptibility measurements vs temperature. The χ_M vs T plot for **1** shows the shape for a weakly antiferromagnetically coupled nickel(II) one-dimensional complex without a maximum until 4 K. In contrast, for complex **2** the shape of the χ_M vs T curve shows a maximum near 40 K, indicating medium antiferromagnetic coupling. From the spin Hamiltonian $-J_{ij}S_iS_j$, J values for **1** and **2** were less than -1 and -29.1 cm^{-1}, respectively. The magnetic behavior for **1** and **2** may be explained in terms of the overlap between magnetic orbitals, taking into account the torsion of the Ni(II) atoms and azido-bridging ligands in the two structures.

Introduction

The azido anion is a versatile bridging ligand which can coordinate Ni(II) ions, giving dinuclear complexes in either end-to-end[2−5] or end-on[6−10] form, tetranuclear complexes in end-on[11] form, 1-D *cis* complexes in end-to-end form,[12,13] 1-D *trans* complexes in end-to-end form (uniform chains[14−16] and alternating chains[17]) or in end-on[10] form, alternating triple end-on and single end-to-end[18] forms, and finally, bidimensional complexes in which both end-to-end and end-on forms are present.[19] In these syntheses the nickel/azido/amine ratio is very important. For bidentate amines and using a 1/1/2 ratio, two kind of complexes are available: dinuclear ferro- or antiferromagnetically coupled systems and *trans* or *cis* 1-D systems with the same empirical formula, $[Ni(\mu\text{-}N_3)L_2]^+$. It is currently impossible to predict what kind of system will be obtained, but the counter anion appears to play an important role. For example, when the amine ligand is the ethylenediamine, it is possible to synthesize an antiferromagnetic dinuclear complex[5] with PF_6^- and a ferromagnetic dinuclear[10] one with ClO_4^- (the cationic part having the same empirical formula). When 1,3-propanediamine and its 2,2′-dimethyl derivative are used, *trans* 1-D antiferromagnetic systems are always obtained[20] with ClO_4^- and

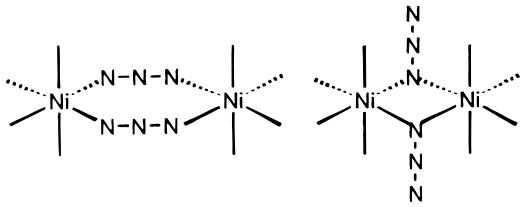

end-to-end *end-on*

⊗ Abstract published in *Advance ACS Abstracts,* January 15, 1996.

(1) (a) Department of Inorganic Chemistry, University of Barcelona. (b) Current address: Department of Chemistry, Burdwan University Burdwan, India. (c) Department of Inorganic Chemistry, University of Pais Vasco. (d) Department of Crystallography, University of Barcelona.
(2) Wagner, F.; Mocella, M. T.; D'Aniello, M. J.; Wang, A. J. H.; Barefield, E. K. *J. Am. Chem. Soc.* **1974**, *96*, 2625.
(3) Pierpont, C. G.; Hendrickson, D. N.; Duggan, D. M.; Wagner, F.; Barefield, E. K. *Inorg.Chem.* **1975**, *14*, 604.
(4) Chaudhuri, P.; Guttman, M.; Ventur, D.; Wieghardt, K.; Nuber, B.; Weiss, J. J. *J. Chem. Soc. Chem. Comm.* **1985**, 1618.
(5) Ribas, J.; Monfort, M.; Diaz, C.; Bastos, C.; Solans, X. *Inorg. Chem.* **1993**, *32*, 3557.
(6) Arriortua, M. I.; Cortés, A. R.; Lezama, L.; Rojo, T.; Solans, X. *Inorg. Chim. Acta* **1990**, *174*, 263.
(7) Escuer, A.; Vicente, R.; Ribas, J. *J. Magn. Magn. Mater*. **1992**, *110*, 181.
(8) Vicente, R.; Escuer, E.; Ribas, J.; Fallah. M. S.; Solans, X; Font-Bardía, M. *Inorg. Chem.* **1993**, *32*, 1920 and references therein.
(9) Cortés, R.; Ruiz de Larramendi, J. I.; Lezama, L.; Rojo, T.; Urtiaga, K.; Arriortua, M. I. *J. Chem. Soc., Dalton Trans.* **1992**, 2723.
(10) Ribas, J.; Monfort, M.; Diaz, C.; Bastos, C.; Solans, X. *Inorg. Chem.* **1994**, *33*, 484.
(11) Ribas, J.; Monfort, M.; Costa, R.; Solans, X. *Inorg. Chem.* **1993**, *32*, 695.
(12) Cortés, R.; Urtiaga, K.; Lezama, L.; Pizarro, J. L.; Goñi, A.; Arriortua, M. I.; Rojo, T. *Inorg. Chem.* **1994**, *33*, 4009.
(13) Ribas, J.; Monfort, M.; Diaz, C.; Bastos, C.; Mer, C.; Solans, X. *Inorg. Chem.* **1995**, *34*, 4986.
(14) Escuer, A.; Vicente, R.; Ribas, J.; El Fallah, M. S.; Solans, X. *Inorg. Chem.* **1993**, *32*, 1033.
(15) Escuer, A.; Vicente, R.; Ribas, J.; El Fallah, M. S.; Solans, X.; Font-Bardia, M. *Inorg. Chem.* **1993**, *32*, 3727.
(16) Escuer, A.; Vicente, R.; Ribas, J.; El Fallah, M. S.; Solans, X.; Font-Bardía, M. *Inorg. Chem.* **1994,** *33*, 1842.
(17) Vicente, R.; Escuer, A.; Ribas, J.; Solans, X. *Inorg. Chem.* **1992**, *31*, 1726.
(18) Ribas, J.; Monfort, M.; Ghosh, B. K.; Solans, X. *Angew. Chem., Int. Ed. Engl.* **1994**, *33*, 2087.
(19) (a) Monfort, M.; Ribas, J.; Solans, X. *J. Chem. Soc., Chem. Commun.* **1993**, 350. (b) Ribas, J.; Monfort, M.; Solans, X.; Drillon, M. *Inorg. Chem.* **1994**, *33*, 742.

0020-1669/96/1335-0864$12.00/0

PF_6^-, while an antiferromagnetic dinuclear complex is obtained[5] with $[B(C_6H_5)_4]^-$. In contrast, working with 2,2′-bipyridine[12] and 1,2-diamino-2-methylpropane,[13] *cis* 1-D complexes are obtained with ClO_4^- and PF_6^-. Focusing our attention on these differences and/or similarities, we have managed to synthesize two new complexes with 2-(aminoethyl)pyridine, working with ClO_4^- and PF_6^-. In this new case, the counteranion effect is again very important; with ClO_4^- a *cis* 1-D system was obtained whereas with PF_6^- a new dinuclear complex has been synthesized. Magnetostructural correlations have been made to compare the new results with the data previously reported for dinuclear or 1-D systems.[2−5,12,13]

Experimental Section

Caution! Perchlorate and azide complexes of metal ions are potentially explosive. Only a small amount of material should be prepared, and it should be handled with caution.

Synthesis of the New Complexes. [Ni(2-(aminoethyl)pyridine)$_2$-(μ-N$_3$)]$_n$(ClO$_4$)$_n$·nH$_2$O (1). To an aqueous solution of 1 mmol (0.365 g) of $Ni(ClO_4)_2·6H_2O$ and 2 mmol (0.244 g) of 2-(aminoethyl)pyridine in 30 mL of water was added an aqueous solution of 1 mmol (0.065 g) of NaN_3. After filtration to remove any impurity, the aqueous solutions were left undisturbed, and well-formed blue crystals of **1** were obtained after several days. The elemental analyses (C, N, H, Ni) were consistent with the formulation. Anal. Calcd/Found: C, 36.35/36.3; H, 4.79/4.8; N, 21.19/21.1; Cl, 7.66/7.6; Ni, 12.69/12.6.

[Ni$_2$(2-(aminoethyl)pyridine)$_4$(μ-N$_3$)$_2$](PF$_6$)$_2$ (2). To an aqueous solution of 1 mmol (0.291 g) of $Ni(NO_3)_2·6H_2O$ and 2 mmol (0.244 g) of 2-(aminoethyl)pyridine in 30 mL of water was added an aqueous solution of 1 mmol (0.065 g) of NaN_3. After filtration to remove any impurity, 1.2 mmol (0.220 g) of KPF_6 was added with continuous stirring. The aqueous solutions were left undisturbed, and well-formed blue crystals of **2** were obtained after several days. The elemental analyses (C, N, H, Ni) were consistent with the formulation. Anal. Calcd/Found: C, 34.31/34.3; H, 4.11/4.2; N, 20.01/20.0; Ni, 11.98/12.0.

Physical Measurements. IR spectra were recorded on a Nicolet 520 FT-IR spectrometer. Magnetic measurements were carried out on polycrystalline samples with a pendulum type magnetometer (MANICS DSM8) equipped with a helium continuous-flow cryostat, working in the temperature range 4−300 K, and a Brucker BE15 electromagnet. The magnetic field was approximately 15 000 G. The instrument was calibrated by magnetization measurement of a standard ferrite. Diamagnetic corrections were estimated from Pascal constants.

Crystal Data Collection and Refinement. Crystals of **1** (0.15 × 0.10 × 0.20 mm) and **2** (0.1 × 0.1 × 0.2 mm) were mounted on an Enraf-Nonius CAD4 four-circle diffractometer. Unit cell parameters were determined from automatic centering of 25 reflections ($12° < \theta < 21°$ for **1** and for **2**]. For **1** 5940 reflections were measured in the range $1.72° < \theta < 29.97°$; 5646 were nonsymmetry equivalent (R_{int} (on I) was 0.024), and 3915 were assumed as observed, applying the condition $I > 2\sigma(I)$. For **2**, 5685 reflections were measured in the range $1.80° < \theta < 29.96°$, 5629 of which were nonequivalent by symmetry (R_{int} (on I) was 0.018), and 4737 of which were assumed as observed, applying the same condition. Three reflections were measured every 2 h as orientation and intensity control; significant intensity decay was not observed. Absorption corrections were not made. The crystallographic data are shown in Table 1. The crystal structures were solved by Patterson synthesis using the SHELXS computer program[21] and refined by full-matrix least-squares method, using the SHELX93[22] computer programs. The function minimized was $\sum w(|F_o|^2 - |F_c|^2)^2$ where $w = (\sigma^2(I) + (k_1P)^2 + k_2P]^{-1}$ and $P = (|F_o|^2 + 2|F_c|^2)/3$; the values of k_1 and k_2 are respectively 0.0787 and 0.6095 for **1** and 0.1115 and 0.4085 for **2**. The values for f, f', and f'' were taken from *International Tables of X-Ray Crystallography*.[23] The extinction coefficients were 0.03(1) for **1** and 0.006(1) for **2**. For **1**, two carbon atoms, C(13) and C(14), and three oxygen atoms of the perchlorate ion were located with a positional disorder. An occupancy factor equal to 0.5 was assumed, according to the height of the Fourier map. In the structure **1** refinement, six hydrogen atoms were located from a difference synthesis, 11 hydrogens were computed and all were refined with an overall isotropic temperature factor, using a riding model for computed hydrogen atoms. For **2**, all hydrogen atoms were located from a difference synthesis and refined isotropically. For **1**, 287 parameters were refined. The maximum shift/esd = 0.06, and the mean shift/esd = 0.00. Maximum and minimum peaks in final difference synthesis were 1.041 and −0.618 e Å^{-3}, respectively. For **2**, 343 parameters were refined. The maximum shift/esd = 1.96, and the mean shift/esd = 0.12. Maximum and minimum peaks in final difference synthesis were 0.826 and −0.757 e Å^{-3} respectively. Final atomic coordinates for **1** and **2** are given in Tables 2 and 3, respectively.

Table 1. Crystallographic Data for *cis*-[Ni(2-(aminoethyl)pyridine)$_2$(μ-N$_3$)]$_n$(ClO$_4$)$_n$·nH$_2$O (**1**) and [Ni$_2$(2-(aminoethyl)pyridine)$_4$(μ-N$_3$)$_2$](PF$_6$)$_2$ (**2**)

	1	**2**
formula	$C_{14}H_{22}ClN_7NiO_5$	$C_{28}H_{40}F_{12}N_{14}Ni_2P_2$
fw	462.55	980.10
T[a]		
space group	$P2_1/a$	$P\bar{1}$
a, Å	8.637(2)	9.139(7)
b, Å	18.9995(7)	10.124(3)
c, Å	12.3093(7)	12.024(2)
α, deg	90	70.407(14)
β, deg	105.92(2)	84.19(2)
γ, deg	90	67.67(4)
V, Å^3	1942.5(5)	969.0(8)
Z	4	1
λ (Mo Kα), Å	0.710 69	0.710 69
d_{calc}, g cm^{-3}	1.582	1.680
μ(Mo Kα), cm^{-1}	11.78	11.56
R[b]	0.0624	0.0473
Rw[c]	0.1728	0.1362

[a] Room temperature. [b] $R = \sum||F_o| - |F_c||/\sum|F_o|$. [c] $R_w = [\sum w(|F_o|^2 - |F_c|^2/\sum w|F_o|^2]^{1/2}$.

Results and Discussion

Description of the Structures. *cis-catena*-[NiL$_2$(μ-N$_3$)]$_n$-(ClO$_4$)$_n$·nH$_2$O (1). The structure of this compound consists of 1-D nickel−azido chains isolated by ClO_4^- anions found in the interchain space. The hydration water molecule is placed at hydrogen bond distances to three atoms (N3 = 2.949 Å, N7 = 3.079 Å, O1′ = 2.962 Å, and O3 = 3.153 Å). In the chain structure each Ni(II) atom is coordinated by two bidentate 2-(aminoethyl)pyridine and two azido ligands in a distorted octahedral *cis* arrangement. A labeled scheme is shown in Figure 1. The main bond lengths and angles are listed in Table 4. Other distances and angles may be found in the Supporting Information. The nickel atom occupies a distorted octahedral environment, formed by two N atoms of the two azido-bridging ligands in *cis* geometry and four N atoms of the two bidentate 2-(aminoethyl)pyridine ligands. The two pyridine rings on each Ni(II) atom are placed perpendicularly. The longest Ni−N distances correspond to the Ni−N (azido) ligands (2.18 Å) whereas the shortest are the Ni−N (nonpyridinic) (2.07−2.08 Å) *trans* with respect to the azido ligand. The other two Ni−N (pyridinic) distances are the same and have an intermediate value (2.131 Å). The Ni−azido angles are Ni−N3−N2(ii) = 126.2° and Ni−N1−N2 = 127.8°. The torsion angle formed by Ni−NNN−Ni (calculated as the angle between the normals to the planes Ni−N1−N2−N3 and Ni(i)−N1−N2−N3) is 57.57°. The

(20) Renard, J. P.; Verdaguer, M.; Ribas, J.; Sterling, W. G. *J. Appl. Phys.* **1988**, *63*, 3538.
(21) Sheldrick, G. M. *Acta Crystallogr*. **1990**, *A46*, 467.
(22) Sheldrick, G. M. *SHELX. A computer program for crystal structure determination*, 1990.
(23) *International Tables for X-ray Crystallography;* Kynoch Press: Birmingham, England, 1976.

Table 2. Atomic Coordinates ($\times 10^4$) and Equivalent Isotropic Displacement Parameters (Å^2 $\times$ 10^3) for **1**[a]

	x	*y*	*z*	*U*(eq)
Ni	1429(1)	1456(1)	1957(1)	31(1)
Cl	4671(2)	−944(1)	3659(1)	60(1)
N(1)	2461(5)	2509(2)	2256(4)	45(1)
N(2)	3243(4)	2802(2)	1754(3)	36(1)
N(3)	−980(5)	1892(2)	1249(3)	44(1)
N(4)	2011(5)	1544(2)	388(3)	38(1)
N(5)	3691(5)	1074(2)	2801(4)	46(1)
N(6)	722(5)	1412(2)	3483(3)	41(1)
N(7)	469(5)	466(2)	1432(4)	48(1)
C(1)	1095(7)	1970(3)	−396(4)	48(1)
C(2)	1330(8)	2076(3)	−1439(4)	60(1)
C(3)	2590(8)	1717(4)	−1697(5)	63(2)
C(4)	3550(7)	1302(3)	−907(5)	57(1)
C(5)	3267(6)	1216(3)	142(4)	42(1)
C(6)	4344(6)	757(3)	1021(5)	54(1)
C(7)	4926(6)	1095(3)	2191(5)	53(1)
C(8)	1069(9)	1973(3)	4162(5)	61(2)
C(9)	456(11)	2071(4)	5083(5)	79(2)
C(10)	−562(9)	1583(14)	5293(5)	75(2)
C(11)	−909(9)	1008(4)	4618(6)	71(2)
C(12)	−258(7)	925(3)	3733(5)	53(1)
C(13)	−338(24)	222(12)	3173(18)	57(5)
C(13′)	−976(27)	330(14)	2825(23)	73(6)
C(14)	182(20)	O(7)	2354(14)	75(4)
C(14′)	−932(12)	261(5)	1884(9)	44(2)
OW	2234(7)	−916(3)	652(4)	78(2)
O(1)	4823(17)	−1584(6)	3157(11)	94(3)
O(1′)	3771(18)	−1474(7)	2941(11)	106(4)
O(2)	4595(13)	−1103(6)	4752(9)	79(3)
O(2′)	6019(52)	−1268(19)	4373(33)	282(15)
O(3)	3314(18)	−483(8)	3222(13)	114(4)
O(3′)	3939(33)	−678(13)	4428(23)	190(9)
O(4)	6070(18)	−586(8)	3554(12)	107(4)
O(4′)	5106(21)	−450(8)	2982(14)	121(5)

[a] *U*(eq) is defined as one-third of the trace of the orthogonalized $\mathbf{U}_{ij}$ tensor.

extension of this torsion in the 1-D system together with the *cis* configurations leads to a double-helicoidal nickel−azido skeleton, as shown in Figure 2.

$[Ni_2(2\text{-(aminoethyl)pyridine})_4(\mu\text{-}N_3)_2](PF_6)_2$ (2). The unit cell contains a dinuclear Ni−Ni dication and two hexafluorophosphate anions. The labeled scheme is shown in Figure 3. The main bond lengths and angles are listed in Table 5. Other distances and angles may be found in the Supporting Information. The nickel atom occupies a distorted octahedral environment, formed by two N atoms of the two azido-bridging ligands and four N atoms of the two bidentate 2-(aminoethyl)pyridine ligands. The two *cis* Ni−N(azido) distances are 2.128 and 2.180 Å, the two shortest distances being the two Ni−N (nonpyridinic) bonds *trans* to the Ni−N (azido) bonds (2.085 and 2.087 Å). The Ni−azido angles are Ni−N1−N2 = 126.7° and Ni(i)−N3−N2 = 123.8°. The dihedral angle δ (which is defined as the angle between the $(N_3)_2$ (least-squares) plane and the N−Ni−N plane) is 34.6°, giving a chairlike structure (Figure 3). As in complex **1**, the two pyridine rings on each Ni(II) atom are perpendicular, and at the same time, the two pyridine rings corresponding to different Ni(II) ions are also perpedicular to each other.

Magnetic Properties. *cis-catena*-$[NiL_2(\mu\text{-}N_3)]_n(ClO_4)_n \cdot nH_2O$ (1). The molar magnetic susceptibility vs *T* of **1** is plotted in Figure 4. The molar susceptibility value (4.152×10^{-3} cm^3 mol^{-1} at room temperature) increases continuously when the temperature decreases (down to 4 K). This continuous increase in the χ_M values without any maximum (at least until 4 K) clearly indicates very weak antiferromagnetic intrachain coupling.

Table 3. Atomic Coordinates ($\times 10^4$, Ni and P $\times$ 10^5) and Equivalent Isotropic Displacement Parameters (Å^2 $\times$ 10^4, Ni $\times$ 10^5) for **2**[a]

	x	*y*	*z*	*U*(eq)
Ni	34600(3)	37867(3)	17052(2)	3321(11)
P	8681(9)	18079(8)	61253(6)	493(2)
N(1)	5794(3)	2994(3)	978(2)	466(5)
N(2)	6512(2)	3733(2)	447(2)	367(4)
N(3)	7278(3)	4434(3)	−72(2)	474(5)
N(4)	4271(2)	5085(2)	2417(2)	380(4)
N(5)	4355(3)	1867(2)	3176(2)	422(4)
N(6)	2583(3)	2538(3)	965(2)	413(4)
N(7)	1279(3)	4626(3)	2446(2)	462(5)
C(1)	3532(3)	6590(3)	2035(2)	448(5)
C(2)	3979(4)	7547(3)	2405(3)	566(7)
C(3)	5250(5)	6937(4)	3180(3)	607(8)
C(4)	6001(4)	5388(4)	3603(3)	536(6)
C(5)	5487(3)	4477(3)	3218(2)	416(5)
C(6)	6242(3)	2792(3)	3713(3)	516(6)
C(7)	5053(4)	2021(3)	4156(2)	503(6)
C(8)	3387(4)	2094(4)	77(3)	547(7)
C(9)	2955(5)	1321(4)	−498(3)	653(8)
C(10)	1623(5)	993(4)	−164(3)	672(9)
C(11)	761(4)	1457(4)	731(3)	578(7)
C(12)	1246(3)	2242(3)	1276(2)	429(5)
C(13)	240(4)	2810(4)	2198(3)	575(7)
C(14)	−87(3)	4449(4)	2027(3)	557(7)
F(1)	2542(4)	841(4)	6809(3)	1132(11)
F(2)	80(5)	2158(5)	7254(4)	1462(17)
F(3)	−709(4)	2795(5)	5425(4)	1465(17)
F(4)	1752(5)	1402(7)	5024(3)	1552(19)
F(5)	454(7)	400(5)	6456(5)	1647(20)
F(6)	1357(5)	3211(4)	5802(7)	2013(31)

[a] *U*(eq) is defined as one-third of the trace of the orthogonalized $\mathbf{U}_{ij}$ tensor.

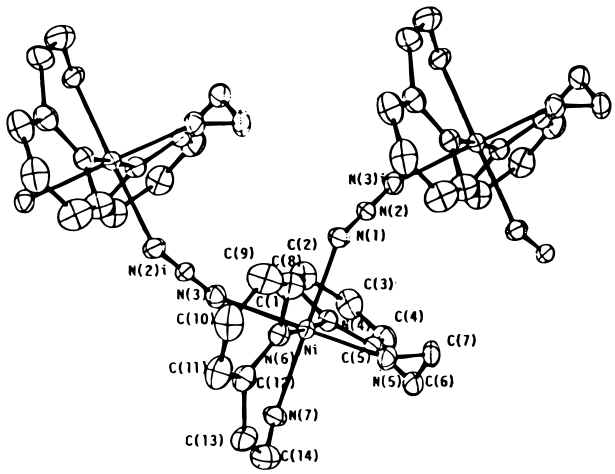

Figure 1. Atom-labeled scheme of the cationic part of *cis-catena*-$[NiL_2(\mu\text{-}N_3)]_n(ClO_4)_n \cdot nH_2O$ (**1**).

Taking into account the single-ion terms and the interactions between the nearest-neighbor center, the more general spin Hamiltonian to describe the magnetic properties of isotropic Ni(II) chains is

$$H = \sum_i (\beta \hat{S}_i \cdot g_i \vec{H} - J \hat{S}_i \cdot \hat{S}_{i+1})$$

The terms corresponding to the anisotropic exchange and antisymmetric exchange have not been considered because these effects are only relevant at very low temperatures (near 2 K).

There is no exact mathematical expression for χ_M vs *T* of infinite isotropic Heisemberg chains. Nevertheless, there are numerical calculations that approximately characterize the Heisemberg behavior in 1-D systems.[24,25] In the case of isotropic 1-D $S = 1$ systems, the temperature dependence of

Table 4. Selected Bond Lengths (Å) and Angles (deg) for *cis*-[Ni(2-(aminoethyl)pyridine)$_2$(μ-N$_3$)]$_n$(ClO$_4$)$_n$ (**1**)[a]

Ni−N(5)	2.076(4)	Ni−N(1)	2.181(4)
Ni−N(7)	2.085(4)	Ni−N(3)	2.186(4)
Ni−N(4)	2.131(4)	N(1)−N(2)	1.173(5)
Ni−N(6)	2.131(4)	N(2)−N(3)(i)	1.185(5)
N(5)−Ni−N(7)	94.5(2)	N(6)−Ni−N(1)	95.1(2)
N(5)−Ni−N(4)	93.3(2)	N(5)−Ni−N(3)	173.7(2)
N(7)−Ni−N(4)	87.9(2)	N(7)−Ni−N(3)	88.0(2)
N(5)−Ni−N(6)	90.2(2)	N(4)−Ni−N(3)	92.5(2)
N(7)−Ni−N(6)	93.0(2)	N(6)−Ni−N(3)	84.0(2)
N(4)−Ni−N(6)	176.4(2)	N(1)−Ni−N(3)	91.1(2)
N(5)−Ni−N(1)	87.2(2)	N(2)−N(1)−Ni	127.8(3)
N(7)−Ni−N(1)	171.7(2)	N(1)−N(2)−N(3)(i)	178.9(4)
N(4)−Ni−N(1)	83.9(2)	N(2)(ii)−N(3)−Ni	126.2(3)

[a] Symmetry transformations used to generate equivalent atoms: (i) $x + {}^1/_2$, $-y + {}^1/_2$, z; (ii) $x - {}^1/_2$, $-y + {}^1/_2$, z.

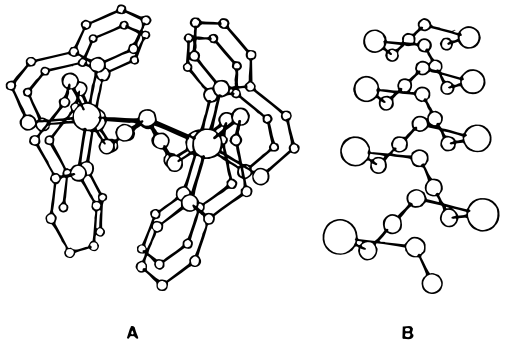

Figure 2. (A) Axial view of the cationic part of *cis-catena*-[NiL$_2$(μ-N$_3$)]$_n$(ClO$_4$)$_n$·*n*H$_2$O (**1**). (B) Helicoidal skeleton of (**1**).

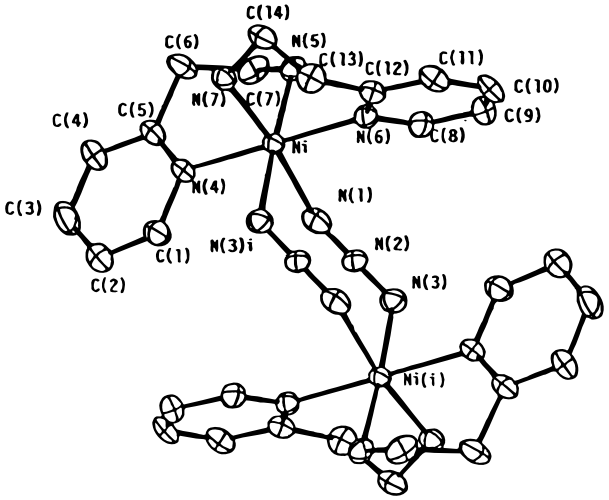

Figure 3. Atom-labeled scheme of the cationic part of [Ni$_2$(2-(aminoethyl)pyridine)$_4$(μ-N$_3$)$_2$](PF$_6$)$_2$ (**2**).

the susceptibility extrapolated from calculations performed on ring systems of increasing length has been given by Weng.[26] Next, the experimental data were fitted to the Weng equation:

$$\chi_M = \frac{N\beta^2 g^2}{kT}\,\frac{2 + 0.019\alpha + 0.777\alpha^2}{3 + 4.346\alpha + 3.232\alpha^2 + 5.834\alpha^3} \qquad \alpha = |J|/kT$$

This formula is only valid for an antiferromagnetic coupling and assuming the nickel ion is magnetically isotropic. A good fit is only possible down to temperatures near the maximum of χ_M (in our case near 4 K). The J values were obtained by

(24) Blöte, H. W. *J. Am. Chem. Soc.* **1964**, *32*, 343.
(25) De Neef, T.; Kuipers, A. J. M.; Kopinga, K. *J. Phys.* **1974**, *A7*, L171.
(26) Weng, C. Y. Ph.D. Thesis, Carnegie Institute of Technology, 1968.

Table 5. Selected Bond Lengths (Å) and angles (deg) for [Ni$_2$(2-(aminoethyl)pyridine)$_4$(μ-N$_3$)$_2$](PF$_6$)$_2$ (**2**)[a]

Ni−N(7)	2.085(2)	Ni−N(1)	2.180(3)
Ni−N(5)	2.087(2)	N(1)−N(2)	1.168(3)
Ni−N(3)(i)	2.128(2)	N(2)−N(3)	1.173(3)
Ni−N(4)	2.153(2)	N(3)−Ni(i)	2.128(2)
Ni−N(6)	2.169(2)		
N(7)−Ni−N(5)	94.35(11)	N(4)−Ni−N(6)	178.30(8)
N(7)−Ni−N(3)(i)	91.84(11)	N(7)−Ni−N(1)	176.29(9)
N(5)−Ni−N(3)(i)	172.58(9)	N(5)−Ni−N(1)	85.75(10)
N(7)−Ni−N(4)	87.75(9)	N(3)(i)−Ni−N(1)	88.33(10)
N(5)−Ni−N(4)	91.89(9)	N(4)−Ni−N(1)	88.54(9)
N(3)(i)−Ni−N(4)	92.44(9)	N(6)−Ni−N(1)	92.52(10)
N(7)−Ni−N(6)	91.19(10)	N(2)−N(1)−Ni	126.7(2)
N(5)−Ni−N(6)	89.52(9)	N(1)−N(2)−N(3)	177.8(2)
N(3)(i)−Ni−N(6)	86.26(9)	N(2)−N(3)−Ni(i)	123.8(2)

[a] Symmetry transformations used to generate equivalent atoms: (i) $-x + 1$, $-y + 1$, $-z$.

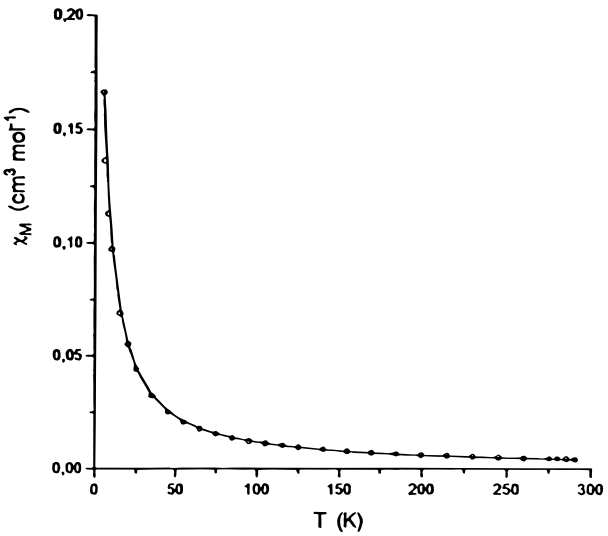

Figure 4. Magnetic susceptibility plots of a polycrystalline sample for *cis-catena*-[NiL$_2$(μ-N$_3$)]$_n$(ClO$_4$)$_n$·*n*H$_2$O (**1**). Solid line shows the best fit (see text).

minimizing the function $R = \Sigma(\chi_M{}^{calcd} - \chi_M{}^{obs})^2/\Sigma(\chi_M{}^{obs})^2$. The best fitted parameters obtained are $0 > J > -1$ cm^{-1}, $g = 2.18$ and $R = 1.2 \times 10^{-4}$.

In previous studies, magnetostructural correlations in end-to-end *trans* and *cis* azido-Ni(II) chains have been reported.[12−16] The three main factors are the Ni−N−N angles, the Ni−NNN−Ni torsion angle, and the Ni−N (azido) distances. By considering first the Ni−N−N angle, the maximum coupling is expected for $\alpha = 108°$. For greater α values (as found experimentally) the antiferromagnetic interaction must decrease. An accidental orthogonality valley, centered on $\alpha = 165°$, was observed. The effect of the Ni−N$_3$−Ni torsion angle was also parameterized. For all α values, the maximum coupling can be expected for a torsion value of zero, decreasing gradually when the torsion angle increases. The magnitude of this effect is lower than the effect of the bond angle. Finally, calculations varying d (Ni−N distance) in the range 2.02−2.20 Å indicate that for greater distances lower antiferromagnetic values occur. For example, a variation of d between 2.09 and 2.21 Å reduced the antiferromagnetic coupling by *ca*. 35%.

In order to explain the weak magnetic coupling of the current 1-D complex (**1**), we have gathered in Table 6 the above mentioned angles and distances together with the J values for all reported 1-D *cis* nickel(II)−azido complexes. In complex **1**, the average Ni−N−N angle is 127°, intermediate between 122° (the lowest) and 151° (the highest). On the other hand,

Table 6. Structural and Magnetic Parameters for *cis* 1-D Complexes of Ni(II) with Azido as the Bridging Ligand

complex	Ni−NNN (deg)	torsion angle (deg)	Ni−N (Å)	J (cm^{-1})	ref
2-methyl[a] with PF_6^-	122.6	53.21	2.174	−3.2	13
	135.0		2.171		
2-methyl[a] with ClO_4^-	125.9	54.10	2.144	−16.8	13
	131.8		2.160		
bipy[b] with ClO_4^-	121.9	46.1	2.123	−33	12
	123.9	41.1	2.086		
bipy[b] with PF_6^-	122.6	45.1	2.100	22	12
	124.0	42.0	2.093		
(3,3,3)[a] with PF_6^-	151.3	37.2	2.164	−18.5	16
	151.8		2.102		
2-ametpy with ClO_4^-	127.8	57.57	2.181	<-1	this work
	126.2		2.186		

[a] 2-methyl = 1,2-diamino-2-methylpropane. [b] bipy = 2,2′-bipyridine. [c](3,3,3) = *N*,*N*′-bis(3-aminopropyl)-1,3-propanediamine.

the Ni−NNN−Ni torsion angle is the highest (57.6°), and the Ni−N distances are the longest (2.18 Å). These two factors considerably diminish the J value. For example, the hexafluorophosphate with 1,2-diamino-2-methylpropane has a torsion angle of 53.2° and a Ni−N distance of 2.17 Å, the experimental J values being -3 cm^{-1}. In the present case, the torsion angle is higher and the Ni−N distance is longer, thus creating an experimental J value less than -3 cm^{-1}. Consequently, the experimental J value (>-1 cm^{-1}) agrees perfectly with all data reported in Table 6.

$[Ni_2(2\text{-(aminoethyl)pyridine})_4(\mu\text{-}N_3)_2](PF_6)_2$ (2). The χ_M vs T plot is shown in Figure 5. The value of χ_M increases to a maximum at 40 K and then decreases. This behavior is typical of an antiferromagnetically coupled Ni(II)−Ni(II) pair. Variable temperature susceptibility data (4−300 K) were analyzed using the isotropic Heisemberg model,[27] in which $H = -JS_1S_2$, assuming a zero field parameter $D = 0$. Least-squares fitting of the magnetic data lead to the following parameters: $J = -29.1$ cm^{-1} and $g = 2.2$.

In a previous work[5] on a series of dinuclear Ni(II) complexes bridged by two azido ligands, we demostrated that the J value is strongly correlated with the dihedral angle δ (as defined above) whereas the distances Ni−N and other angles have less importance. For a dihedral angle of 45°, the J value is -4.6 cm^{-1}; for $\delta = 20.7°$, J is -70 cm^{-1}; and for $\delta = 3.0°$, J is -114.5 cm^{-1}. In the current case, δ is 34.6°, and the J value $= -29.1$ cm^{-1}, intermediate between -4.6 and -70 cm^{-1}. Consequently, this complex (**2**) is a new one which can be added with perfect agreement to the series previously reported for similar complexes.[5]

(27) O'Connor, C. J. *Prog. Inorg. Chem.* **1982**, *29*, 239.

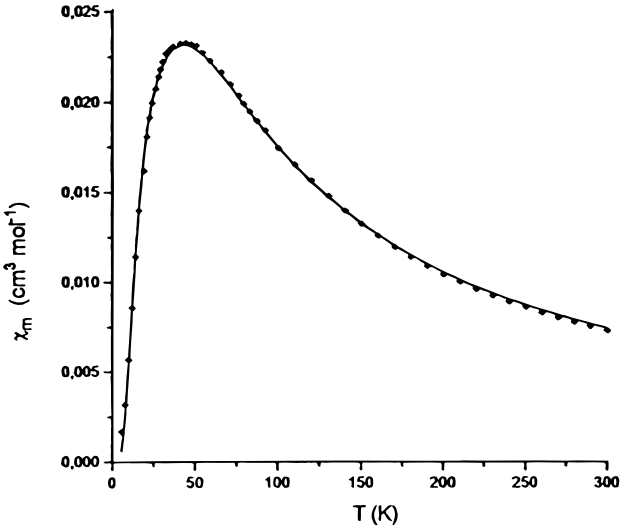

Figure 5. Magnetic susceptibility plots of a polycrystalline sample for $[Ni_2(2\text{-aminoethylpyridine})_4(\mu\text{-}N_3)_2](PF_6)_2$ (**2**). Solid line shows the best fit (see text).

Conclusions

In summary, the magnetic behavior of the two complexes agrees completely with the results previously reported for two similar series. The question which arises is why, in the current case, the perchlorate gives a 1-D complex while the hexafluorophosophate gives a dinuclear complex. Until now, we could not explain this feature; it is even harder to explain when we take into account that with 2,2′-bipyridine and 1,2-diamino-2-methylpropane both ClO_4^- and PF_6^- give *cis* 1-D complexes which are very similar to each other.[12,13] Until now the results obtained seem to indicate a correlation between the size and substituent of amine and the size of the counteranion, which forces a different kind of packing in each case. New experiments and results are necessary in order to clarify this unexpected behavior. Current efforts are underway in our group to establish their causes.

Acknowledgment. We are very grateful for the financial assistance from the CICYT (Grant PB93-0772). B.K.G. also aknowledges the scholarship accorded by the Spanish Government.

Supporting Information Available: Tables giving crystal data and details of the structure determination, anisotropic thermal parameters, bond angles and distances, and hydrogen atoms coordinates (29 pages). Ordering information is given on any current masthead page.

IC9510573